Natural Resources Canada | Ressources naturelles Canada

GEOLOGICAL SURVEY OF CANADA
OPEN FILE 8849

Hydrogen sulfide (H_2S) distribution in the Triassic Montney Formation of the Western Canadian Sedimentary Basin

A.W. Kingston, A. Mort, C. Deblonde, and O.H. Ardakani

2021

Canada

GEOLOGICAL SURVEY OF CANADA
OPEN FILE 8849

Hydrogen sulfide (H_2S) distribution in the Triassic Montney Formation of the Western Canadian Sedimentary Basin

A.W. Kingston, A. Mort, C. Deblonde, and O.H. Ardakani

2021

Permanent link: https://doi.org/10.4095/329266

This publication is available for free download through GEOSCAN (https://geoscan.nrcan.gc.ca/).

Recommended citation
Kingston, A.W., Mort, A., Deblonde, C., and Ardakani, O.H., 2021. Hydrogen sulfide (H_2S) distribution in the Triassic Montney Formation of the Western Canadian Sedimentary Basin; Geological Survey of Canada, Open File 8849, 21 p. https://doi.org/10.4095/329266

Publications in this series have not been edited; they are released as submitted by the author.

Table of Contents

ABSTRACT

The Montney Formation is a highly productive hydrocarbon reservoir that is of great economic importance to Canada, however production is often dogged by the presence of hydrogen sulfide (H_2S), a highly toxic and corrosive gas. Mapping H_2S distribution across the Montney basin in the Western Canadian Sedimentary Basin (WCSB) is fundamental to understanding the processes responsible for its occurrence. We derive a Montney-specific dataset of well gas and water geochemistry from the publically available archives of the Alberta Energy Regulator (AER) and British Columbia Oil and Gas Commission (BCOGC) conducting quality assurance and control procedure before spatial interpolation. Empirical Bayesian Kriging is used to interpolate H_2S across the whole Montney basin resulting in maps of H_2S from hydrocarbon gas, condensates, and water; along with maps of sulfate and chloride ions in water. These interpolations illustrate the heterogeneous distribution of H_2S across the basin with the highest concentrations in the Grande Prairie area along with several other isolated regions. Maps of H_2S in gas, condensates, and water exhibit similar trends in H_2S concentrations, which with future research may help elucidate the origin of H_2S in the Montney.

INTRODUCTION

Hydrogen sulfide (H_2S) is a toxic and corrosive gas, which poses significant risks to both human and environmental health even in concentrations as low as 1 ppm (Canadian Centre for Occupational Health and Safety). In addition, its corrosive nature and reduction of the calorific value of extracted hydrocarbons (Desrocher, 1997) negatively impacts the economics of hydrocarbon development. H_2S occurs naturally in many hydrocarbon reservoirs with a broad range of concentrations and regional variability (e.g. Hutcheon, 1999). Therefore, accurate prediction of subsurface H_2S occurrence is essential to reduce the risk of encountering high H_2S unexpectedly and minimize hazardous exposure.

The Lower Triassic Montney Formation (Fm.) is a dolosiltstone sequence within the Western Canadian Sedimentary Basin (WCSB) stretching across northwestern Alberta and northeastern British Columbia. The Montney Fm. is a prolific tight gas reservoir, which continues to undergo significant development. The amount of marketable reserves in the Montney Fm. are estimated to be 12,719 Gm^3 of natural gas, 2,308 Mm^3 of natural gas liquids, and 179 Mm^3 of oil (National Energy Board, 2013) and therefore is of significant economic interest to Canada.

Previous studies of H_2S concentrations within the Triassic formations of the WCSB indicate that concentrations range from 0–29% with significant regional variability (Kirste et al., 1997; Desrocher et al., 2004). However, the proliferation of hydrocarbon development in the Montney Fm. coupled with significant increases in available data within provincial archives provides an excellent opportunity to revisit the mapping of H_2S distribution. Recent work by Chalmers et al. (2020) mapped H_2S within the Montney Fm. using data within the geoSCOUT GIS software (geoLOGIC Ltd., 2019) showing a range in concentration from <100-210,000 ppm and large spatial heterogeneities in the distribution. This Open File Report expands on previous work by: (a) extending the map across the whole Montney basin; (b) utilizing stratigraphic models developed by provincial regulators to filter out Montney specific data using 3D locational information; and (c) classifying and mapping H_2S content in discrete liquid, gas, and aqueous phases.

Furthermore, in order to better understand the potential processes responsible for H_2S formation in the subsurface, the distribution of sulfate (SO_4) and chloride (Cl) is evaluated. It is well established that dissolved sulfate and hydrocarbons are thermodynamically unstable in diagenetic environments and reduction of sulfate is the main process responsible for high H_2S concentrations (Worden and Smalley, 1996; Machel, 2001). Chloride is a conservative ion that is useful to assess where sulfate reduction has occurred; helping track changes in subsurface sulfur cycling.

This report presents a series of maps of H_2S distribution within the Montney Formation from several different sample phases, (a) gas-phase, (b) liquid-phase, and (c) in the aqueous phase. Along with these are maps of aqueous sulfate (SO_4) and chloride (Cl) concentrations, which are relevant to understanding H_2S formation processes in the subsurface.

METHODS

Data Resources

Provincial regulators require operators to report compositional analysis of hydrocarbon and water samples (including H_2S and other relevant geochemical species) to provincial databases that are maintained by the respective regulator. These data are publically available for Alberta from the Alberta Energy Regulator (AER) and for British Columbia from the British Columbia Oil and Gas

Commission (BCOGC). All data for the maps in this report were derived from these data archives. The data in this report were current as of December 2020.

Note that the Alberta Geological Survey has published an H_2S digital data release (Lyster, 2020) that includes H_2S values from well tests in the Montney and adjacent formations in Alberta. This digital data release was not incorporated into this report since it largely represents a duplication of the source data obtained from AER.

Montney 3D Model

The recent availability of a 3D spatial subsurface model for the Montney, published by the Alberta Geological Survey (AGS) (Lyster et al., 2020) enables the stratigraphy of point data to be allocated according to their position in 3D space. The AGS 3D Montney model has been extended into North East British Columbia (NEBC) to form a coherent depth structure model across the whole of the Montney basin (Mort et al., 2021; in prep.). The spatial locations for the gas samples in deviated and horizontal wellbores, which make up the majority of modern (2006-present) Montney wells have been corrected via directional survey data to form a 3D cloud of data points projected in the subsurface (Fig. 1). Using this method of data filtering via its true location within the model removes potential errors associated with: (a) inaccurate reporting of targeted formations; (b) inaccurate reporting of targeted pools; and (c) permits the inclusion of values without reported formations or pools, which greatly increases the size of the database and the quality of the interpolations. The resulting output was the basis for all subsequent quality assurance and quality control processes.

Quality Assurance Processing

For quality assurance purposes a standardized workflow was developed within FME™ (Safe Software) to efficiently filter out records from AER and BCOGC's large data archives and constrain the dataset to Montney-specific records for further evaluation and validation. FME™ provides data transformation capabilities that enabled an iterative QA/QC process involving data selection/rejection and the creation of minimum, maximum, median, standard deviation and sample count statistics for the various elements at each x, y data points, which are then exported to ArcGIS for spatial analysis. The QA/QC process consisted of removing extreme values based on histograms (i.e. outliers), different data types (e.g. binary vs. continuous), and checking

spatially isolated extreme values. The FME™ workflow for the water dataset is shown in Fig. 2. Components of the specific filters are described in detail below.

First Montney records were identified and extracted from the entire dataset (representing roughly 27,000 samples out of a total of ~400,000) using corrected location criteria fro classification as described in 3D Montney modelling section. Then all wells without reported Kelly Bushing (KB) datum values were removed due to potential inaccuracies in calculating true vertical depth. This resulted in the removal of 20 wells from the hydrocarbon dataset and two wells from the water dataset. All wells listed as injection and disposal wells were removed: this includes acid gas injection, acid gas disposal, and water injection wells as listed in the Well Status. These wells were removed as the reported chemistry is unlikely to reflect connate formation chemistry. This resulted in the exclusion of 75 wells for the gas dataset and 15 wells from the water chemistry dataset.

Finally hydrocarbon gas data was classified by phase as either gas or condensate here termed: gas-phase and liquid-phase; in an attempt to understand distribution of H_2S in a multiphase system. Fluid samples with a plus fraction (heptane and heavier components; C7+) in excess of 0.1 mol% were classified as liquid-phase (condensates) and samples with C7+ values less than 0.1 mol% were classified as gas-phase. We recognise that the partition of H_2S into discrete phases is a function of separator condition rather than representing mono- or diphasic reservoir fluids but our approach does acknowledge these artefacts and attempts to address the partition of produced H_2S according to phase.

Quality Control Processing

Following quality assurance procedures described above quality control was preformed on the dataset to remove spurious, inaccurate, and/or values not indicative of formation fluids. Often this is related to anomalous stratigraphic provenance, sampling locations, or comingling of fluids from multiple depths in a well. These filters differed between the gas and water databases as shown below.

All Data

(1) The 50 highest values for each species (e.g. H_2S, SO_4, etc.) were assessed to ensure they were reflective of formation fluids and not anomalous. Several values were found to have errors in reporting of H_2S values, or from commingled wells, these values were excluded.

(2) Records classified as Montney according to the depth structure model (Mort et al., in prep) with designated Pool names not in agreement with Montney Pools were flagged and removed as a conservative measure to maintain the integrity of the interpretation, such that samples of ambiguous provenance (e.g. Belloy, Taylor Flats, Buick Creek etc. Pool samples interpreted as Montney in the 3D model) would not spuriously influence the mapping of H_2S concentration data. This includes pools designated as "commingled" or equivalent.

Water Dataset

(1) For H_2S in water interpolation: all data reported from Maxxam Analytics were excluded (n = 1617) as the data was binary (i.e., a 0 represents "not present" and 1 represents "present") and not reflective of real continuous concentration values.
(2) For SO_4 in water interpolation: values greater than 5,000 mg/L were excluded (n = 25) as these are extremely high sulfate concentrations for formation waters and many of the sample locations suggest they would not be accurate representations of formation water chemistry (e.g., sampling location = "bottom of storage tank").
(3) For Cl in water interpolation: one value (850,000 mg/L) was removed as it was an extreme outlier compared to the rest of the dataset.

Following these filtering techniques the number of values input into the interpolation were: 19,561 H_2S (gas-phase) values, 7,890 H_2S(liquid-phase) values, 6,293 H_2S(aq) values, 7,753 SO_4(aq) values, and 7,775 Cl(aq) values. Following statistical analysis of these values at each x, y point the total number of x, y points used in the interpolation were: 8,025 H_2S(gas-phase); 3592 H_2S(liquid-phase); 4,055 H_2S(aq); 4,318 SO_4(aq); and 4,331 Cl(aq).

Interpolation of Data, Mapping, and Prediction Error Statistics

Empirical Bayesian Kriging within the Geostatistical Analyst toolbox in ArcGIS Pro 2.8 was used to generate interpolation models of each geochemical species across the Montney basin. Spatial interpolation modeling utilized a single set of values for each x, y location. Individual values for each x, y location were derived from the statistical analysis of the filtered data (workflow detailed above). This resulted in multiple values from a single well (e.g. time or depth series) or different wells with the same x, y position being combined for statistical analysis. For maps of H_2S concentration in gases (Fig. 3 and 4) and H_2S concentration in water (Fig. 5) the maximum value

for each x, y position was used for interpolation. For sulfate (SO_4) concentration in water (Fig. 6) the minimum value for each x, y position was used in an attempt to remove potential artifacts related to artificial increases in sulfate concentrations in flowback water as a result of the hydraulic fracturing process (e.g., Osselin et al., 2019). For chloride (Cl) concentration in water (Fig. 7) the median value for each x, y position was used for interpolation.

The properties of the Empirical Bayesian Kriging interpolations were kept consistent between all maps (Fig. 3 to 7) and were as follows:

Subset Size: 100
Overlap Factor: 1.0
Number of Simulations: 100
Output Surface Type: Prediction
Transformation: None
Semivariogram Type: Power
Neighborhood Type: Smooth Circular
Smoothing Factor: 1.0
Radius: 10,000m

To quality of the model was evaluated via cross-validation using a series of prediction error statistics. This included comparing different geostatistical models (nearest neighbour, inverse distance weighting, kriging, and empirical Bayesian kriging); ensuring the average standard error was similar to the root mean squared prediction errors; and ensuring the percentage of points within the 90% and 95% cross validation confidence interval were close to 90 and 95 respectively. The large size of these geochemical databases and spatial heterogeneities result in occasional instances where the model either under or over predicts the measured value. These model artifacts are assessed spatially using uncertainty maps detailed below.

Interpolation Model Uncertainty Maps

There are several main sources of potential uncertainty for these maps, including: (a) uncertainty in analytical work or data quality related errors; (b) errors related to sampling density; (c) locational errors associated with uncertainty in the stratigraphic model (these include data quality and structural complexity related errors); and (d) geostatistical uncertainty associated with multiple wells/values being averaged for each surface x, y location. Analytical and data quality uncertainty is difficult to quantify owing to different sampling and analytical systems used for individual data points and therefore it is acknowledged as a potential limitation of this series of maps. Uncertainty related to sampling density is caused by operators targeting hydrocarbon-rich units resulting in uneven sampling, however this is the source of our data and beyond our control.

Locational errors due to stratigraphic uncertainty are inherent to 3D modeling and will decrease/improve as more data is built into the model. Geostatistical related uncertainty can be calculated more quantitatively than other sources of error and is therefore addressed below. For each interpolation (H_2S(gas-phase), H_2S(liquid-phase), H_2S(aq), SO_4(aq), Cl(aq)) three measures of model accuracy were calculated: the standard deviation of multiple values for a single surface x, y location, the difference between model predicted values and measured values, and the standard error of the interpolation model.

Standard Deviation Maps

Many x, y locations within the model include values from several different wells and/or multiple values from a single well (e.g. historical time series or depth series). For data interpolation a single set of values is required for each x, y location in the model and therefore either the maximum (H_2S), minimum (SO_4), or median (Cl) values was used for geostatistical analysis. Standard deviations for individual surface x, y points are calculated to show the degree of heterogeneity at individual x, y locations. The number of values averaged for x, y locations ranged from n=1–42 values for H_2S in the hydrocarbon gas-phase, from n=1–19 in the hydrocarbon liquid-phase, and from n=1–31 values for water species (H_2S, SO_4, Cl). In general, standard deviations are low, however, higher standard deviations are typically associated with regions of higher concentration of the geochemical species, indicating a large range in concentration at these points. This could be related to historical variability in H_2S over time, or sampling at different depths within the same well. Assessing the cause of large deviations is beyond the scope of this report and should be the topic for future research. Maps of standard deviations for each x, y location are shown in figures 8a-12a.

Interpolation uncertainty map

To assess and visualize uncertainty in the interpolation model output, a map has been generated to illustrate: (a) the difference between the model prediction values and measured values; and (b) present the standard error of the interpolation model. The standard error of the interpolation model is displayed as a surface, which is calculated using the standard deviation of the estimated value at each x, y location as calculated by the ArcGIS Pro Geostatistical Analyst Toolbox. Maps of the difference between measured and predicted values are displayed as point data overtop of the standard error surface in figures 8b-12b.

RESULTS and PRELIMINARY OBSERVATIONS

Results of the interpolations are shown in figures 3-7. Maps of uncertainty are shown in figures 8-12.

Initial observations reveal the heterogeneous distribution of H_2S across the basin with a major area of high H_2S centred around the Grande Prairie region. Several other areas with high H_2S occur north of Fort St. John in BC and the southeastern portion of the basin near Whitecourt, AB. Comparison of the maps of H_2S in gas-phase, liquid-phase, and water illustrate broad similarities in H_2S distribution.

The spatial distribution of standard deviations in values at each x, y location (Figs. 8a-12a) show that the regions with the highest H_2S concentrations also have the highest standard deviations, which indicates significant local heterogeneities in H_2S distribution. This is consistent with all H_2S maps (e.g. gas-phase, liquid-phase, and water), however is less prevalent in the other geochemical species (SO_4 and Cl). The difference between measured and predicted values and standard error for the interpolations (Fig. 8b-12b) show similar trends to standard deviations with the largest model errors occurring in the regions of the highest H_2S concentration. Again this is thought to be the result of small scale variability in H_2S.

These results highlight the need to assess H_2S distribution at both large and small scales in order to better understand the processes responsible for its occurrence. Future work should attempt to sub-divide the Montney into its lower, middle, and upper submembers (using Davies et al., 2018 subdivision definitions) and look at potential sources of migrated H_2S from major sulfur sources such as the Leduc and Charlie Lake Formations.

REFERENCES

Canadian Centre for Occupational Health and Safety. 2021-10-08. Hydrogen Sulfide. https://www.ccohs.ca/oshanswers/chemicals/chem_profiles/hydrogen_sulfide.html.

Chalmers, G.R.L., Bustin, R.M. and Bustin, A.A., 2020. Hydrogen sulphide within the Triassic Montney Formation, northeastern British Columbia and northwestern Alberta (NTS083K–N, 084C–F, 093I, J, O, P, 094A, B, G, H); in Geoscience BC Summary of Activities 2019: Energy and Water, Geoscience BC, Report 2020-02, p. 41–52.

Davies, G.R., Watson, N., Moslow, T.F. and MacEachern, J.A., 2018. Regional subdivisions, sequences, correlations and facies relationships of the Lower Triassic Montney Formation, west-central Alberta to northeastern British Columbia, Canada—with emphasis on role of paleostructure. Bulletin of Canadian Petroleum Geology, 66(1), 23–92.

Desrocher, S., 1997. Isotopic and compositional characterization of natural gases in the Lower and Middle Triassic Montney, Doig and Halfway Formations, Alberta Basin. Unpublished MSc thesis. Department of Geology and Geophysics, University of Calgary. 202 pp.

Desrocher, S., Hutcheon, I., Kirste, D., Henderson, C.M., 2004. Constraints on the generation of H_2S and CO_2 in the subsurface Triassic, Alberta Basin, Canada. Chemical Geology 204, 237–254.

FME Software. Copyright© Safe Software Inc. www.safe.com

Hutcheon, I., 1999. Controls on the distribution of non-hydrocarbon gases in the Alberta Basin. Bulletin of Canadian Petroleum Geology, 47(4), 573–593.

Kirste, D., Desrocher, S., Spence, B., Hoyne, B., Tsang, B., Hutcheon, I., 1997. Fluid flow, water chemistry, gas chemistry, and diagenesis in the subsurface Triassic in Alberta and British Columbia. Bulletin of Canadian Petroleum Geologists. 45, 742–764.

Lyster, S.; Brown, L. and Playter, T.L., 2020. 3D property model of the Montney Formation in Alberta, version 2 (methodology, model, dataset, multiple files); Alberta Energy Regulator / Alberta Geological Survey, AER/AGS Model 2020-03.

Lyster, S., 2020. Hydrogen Sulphide (H_2S) Concentrations From Gas Analysis Tests in the Montney and Adjacent Formations (tabular data, tab-delimited format); Alberta Energy Regulator / Alberta Geological Survey, AER/AGS Digital Data 2020-0011.

National Energy Board (NEB), 2013. Canada's Energy Future 2013, Energy Supply and Demand Projections to 2035, an Energy Market Assessment November 2013. pp. 87.

Osselin, F., Saad, S., Nightingale, M., Hearn, G., Desaulty, A-M., Gaucher, E.C., Clarkson, C.R., Kloppmann, W., Mayer, B., 2019. Geochemical and sulfate isotopic evolution of flowback and produced waters reveals water-rock interactions following hydraulic fracturing of a tight hydrocarbon reservoir. Science of the Total Environment 687, 1389–1400.

Worden, R.H., Smalley, P.C., 1996. H_2S-producing reactions in deep carbonate gas reservoirs: Khuff Formation, Abu Dhabi. Chemical Geology 133, 157–171.

FIGURES

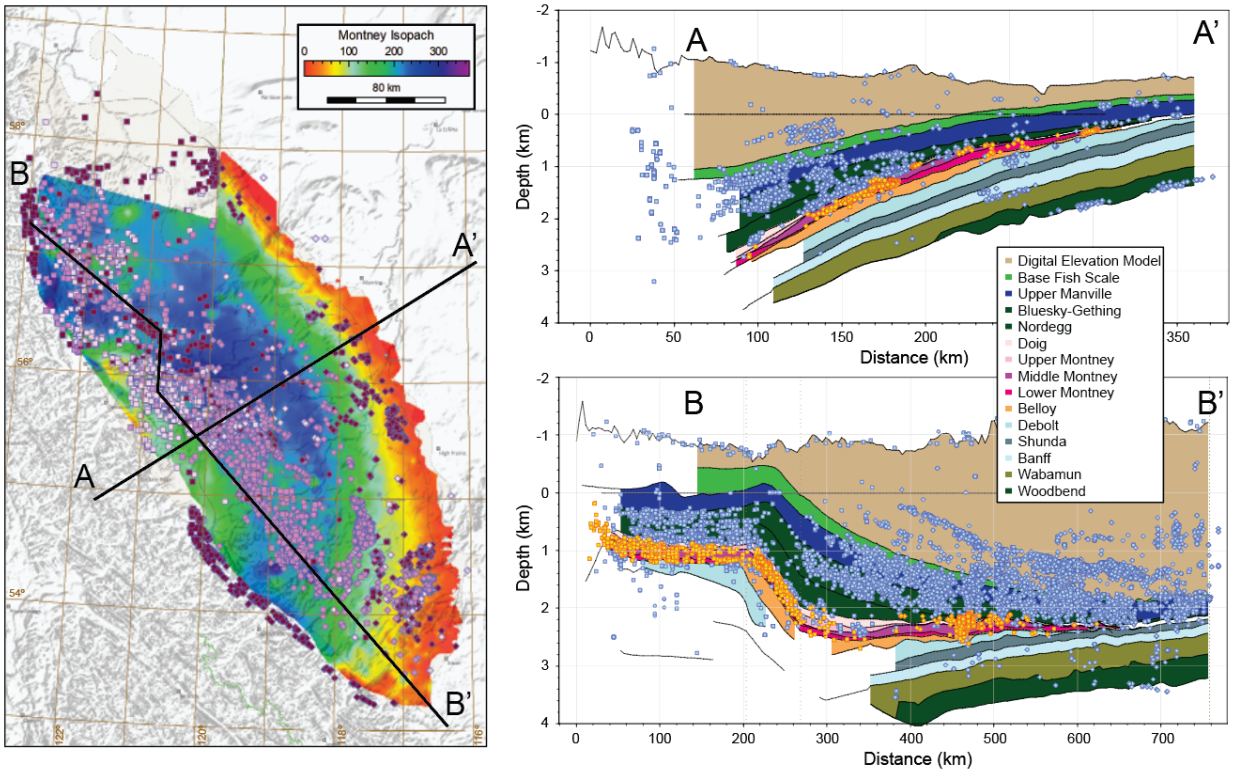

Figure 1. 3D Montney model showing east-west dip (A-A') and strike (B-B') cross-sections with fluid data identified as belonging to the Montney Fm. shown as orange symbols.

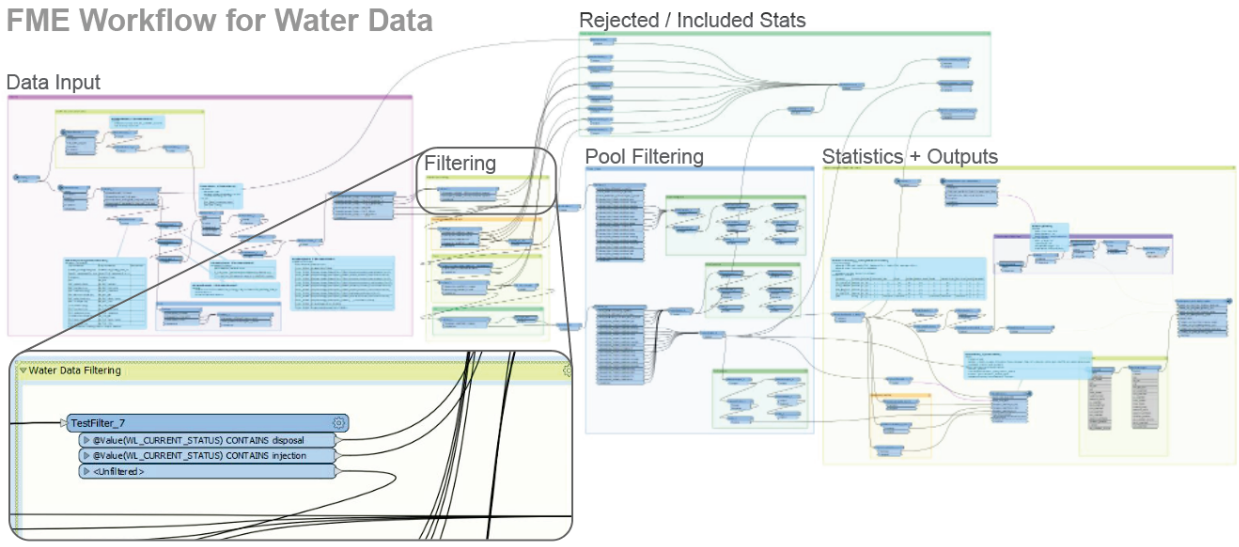

Figure 2. FME workflow used for filtering water data from AER and BCOGC data archives and subsequent statistical analysis of filtering outputs. Enlargement shows details of the main data filtering processes.

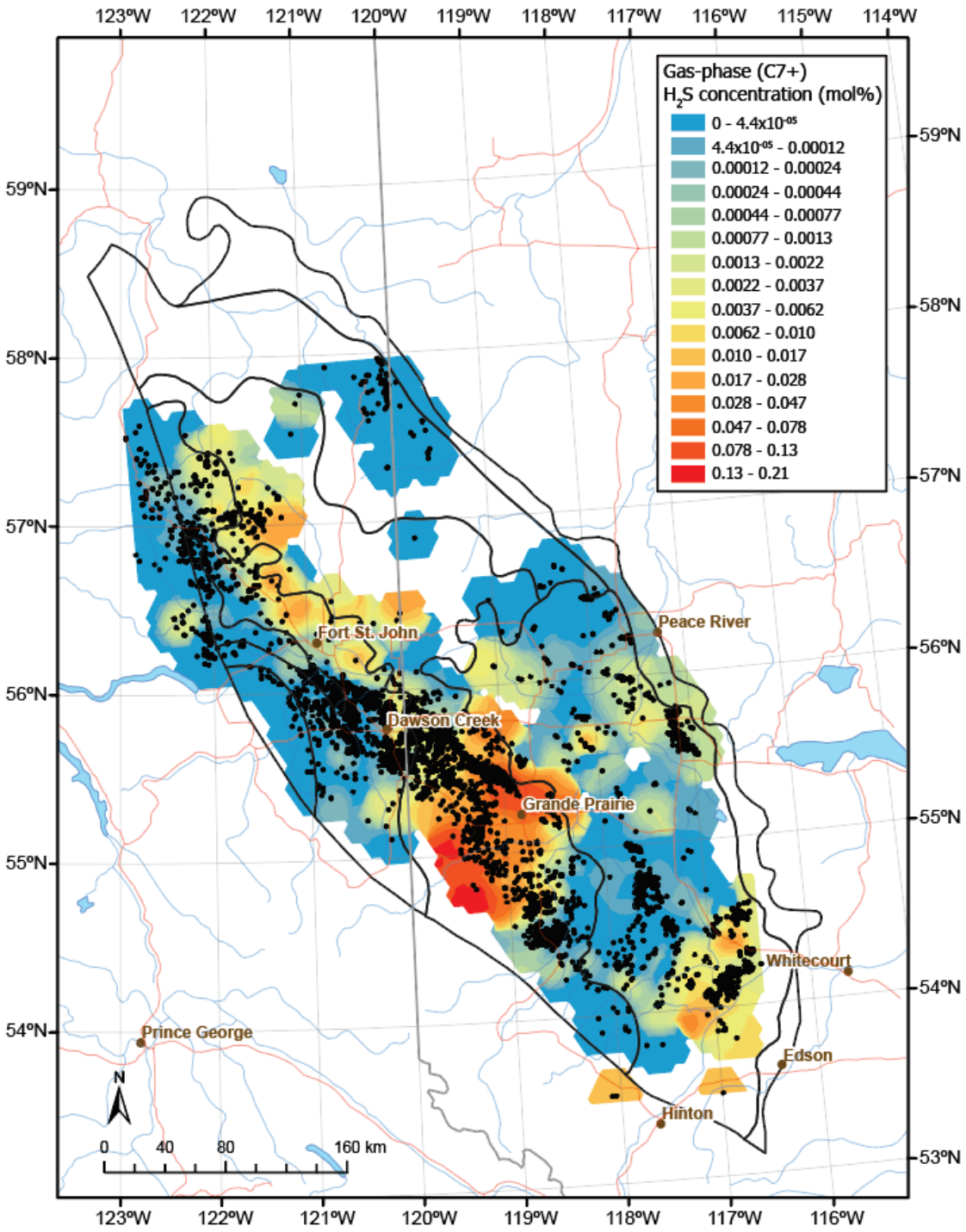

Figure 3. Hydrogen sulfide (H_2S) concentration in the gas-phase. Gas-phase samples are defined as those with a C7+ value lower than 0.1 mol%. Maximum H_2S concentrations were calculated for each surface X-Y location for interpolation.

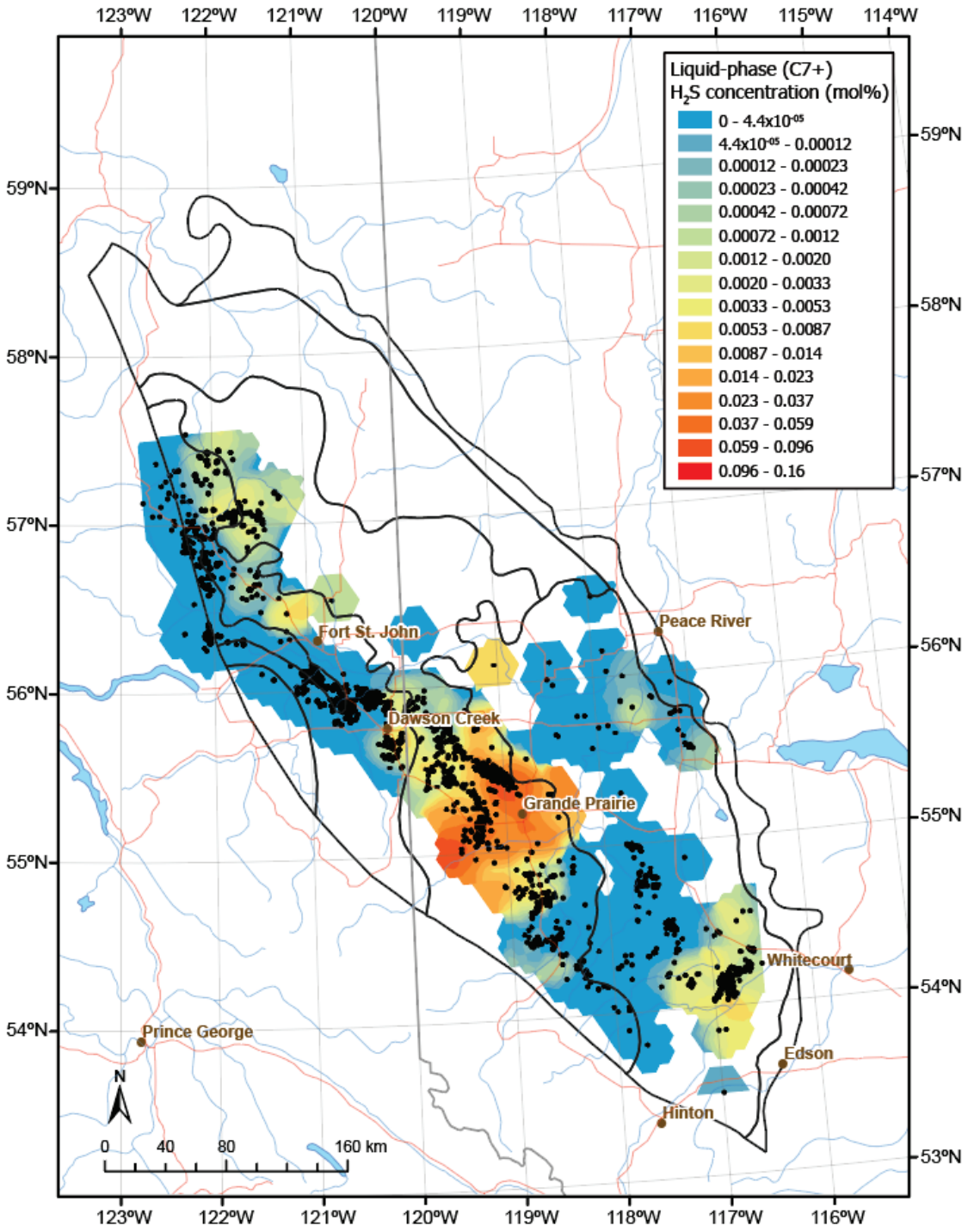

Figure 4. Hydrogen sulfide (H_2S) concentration in the liquid-phase. Liquid-phase samples are defined as those with a C7+ value equal to or greater than 0.1 mol%. Maximum H_2S concentrations were calculated for each surface X-Y location for interpolation.

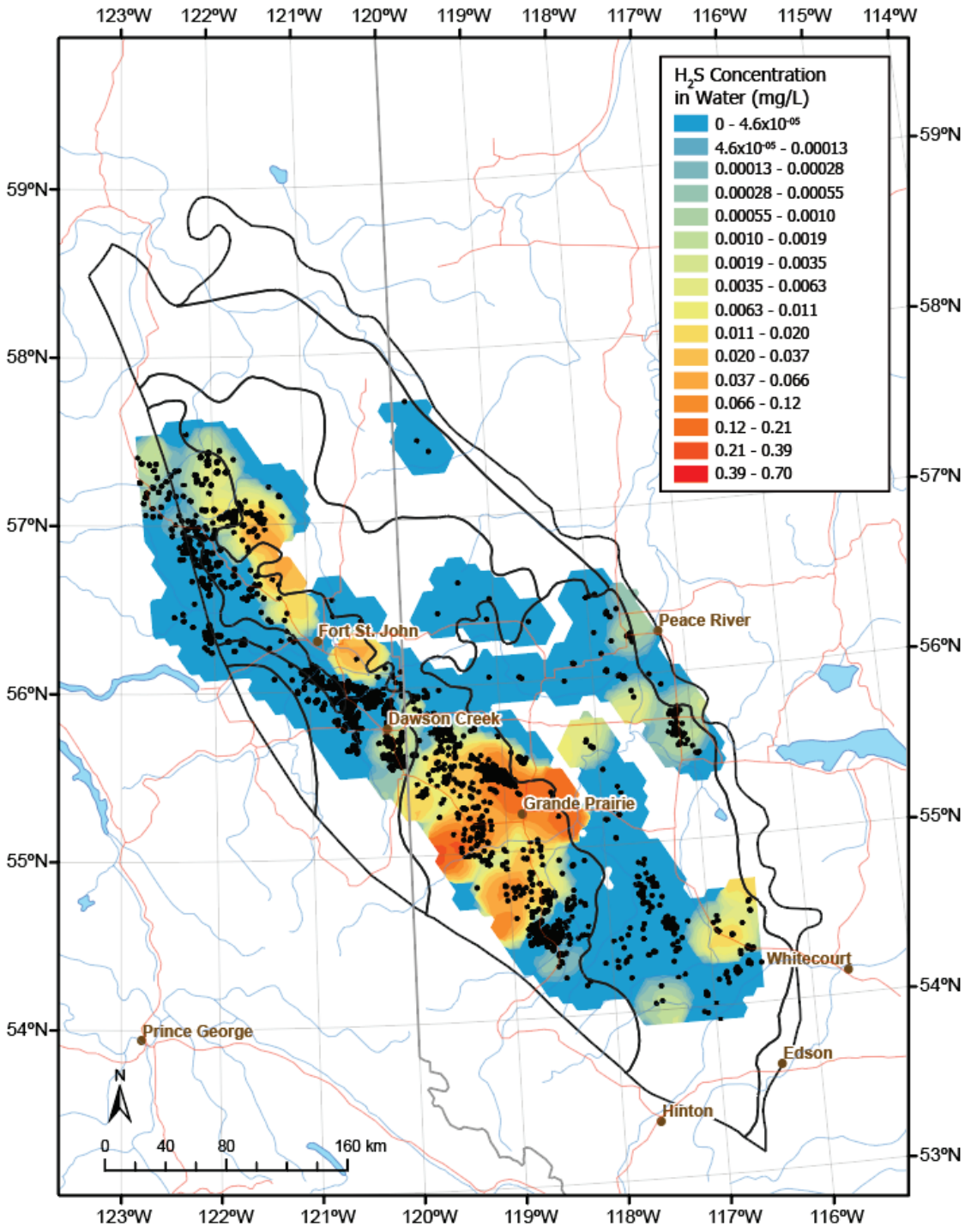

Figure 5. Hydrogen sulfide (H_2S) concentration in the aqueous phase. Maximum H_2S concentrations were calculated for each X-Y point and used for interpolation, see text for details.

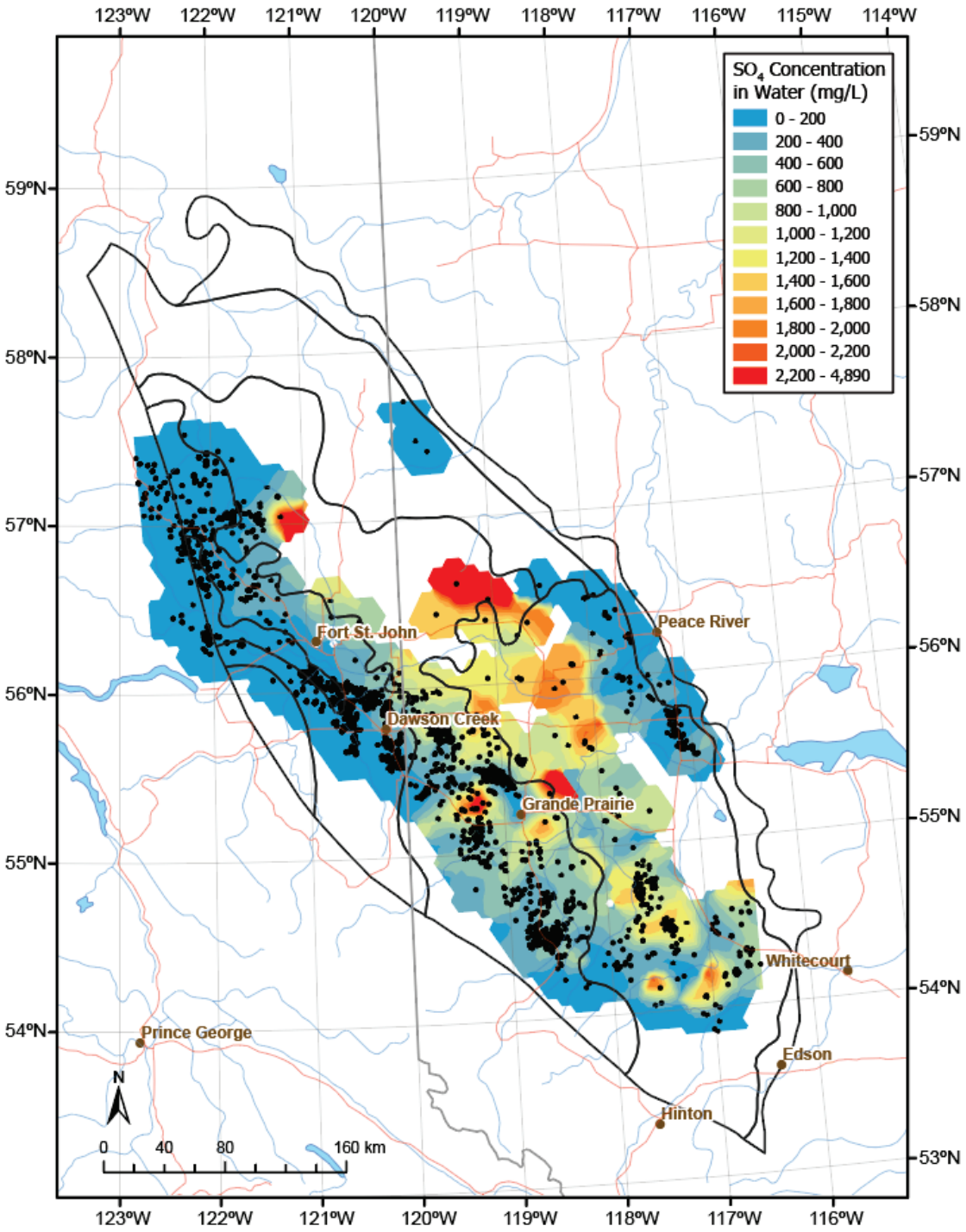

Figure 6. Sulfate (SO_4) concentration in water. Minimum SO_4 concentrations were calculated for each X-Y point and used for interpolation, see text for details.

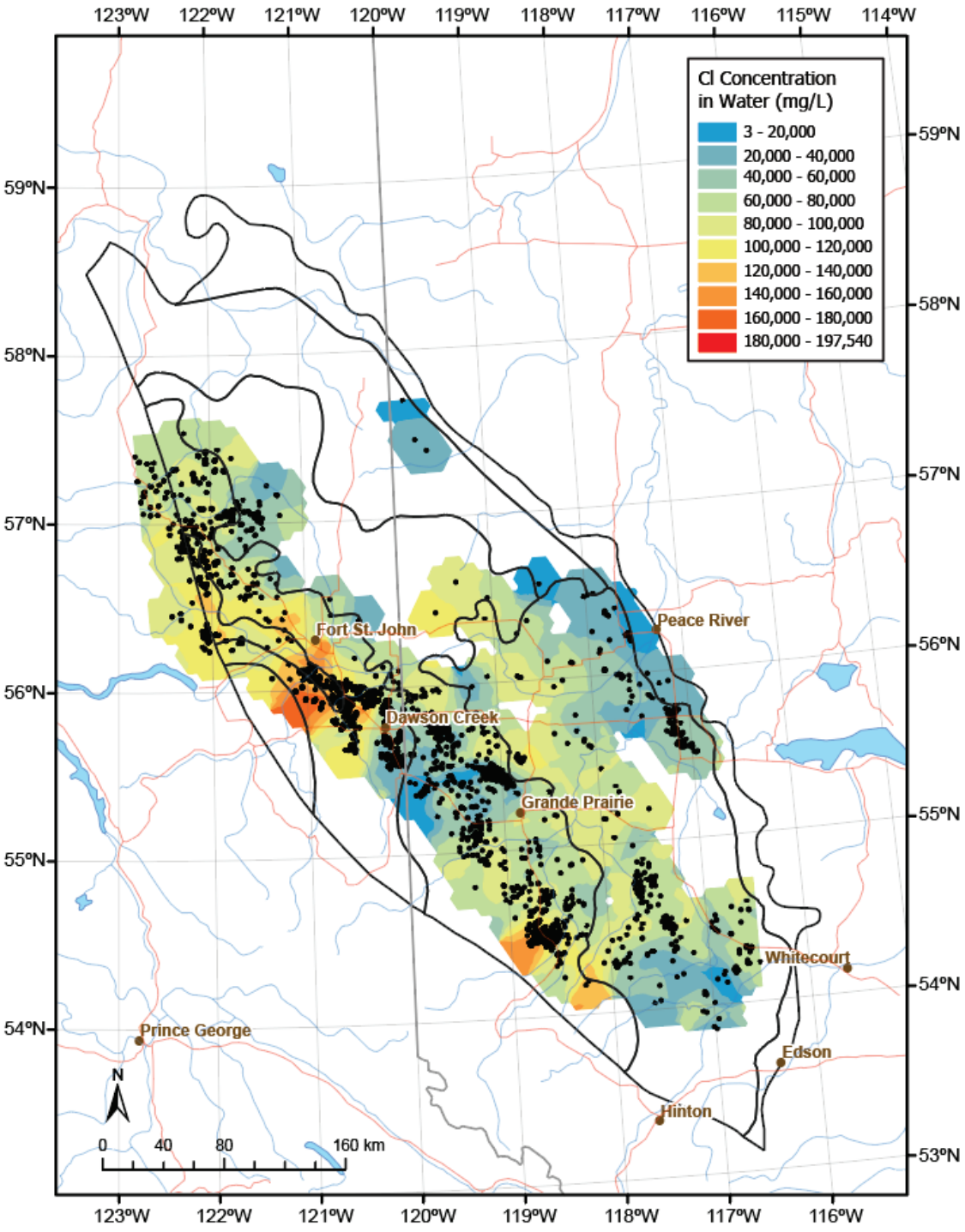

Figure 7. Chloride (Cl) concentration in water. Median Cl concentrations were calculated for each X-Y point and used for interpolation, see text for details.

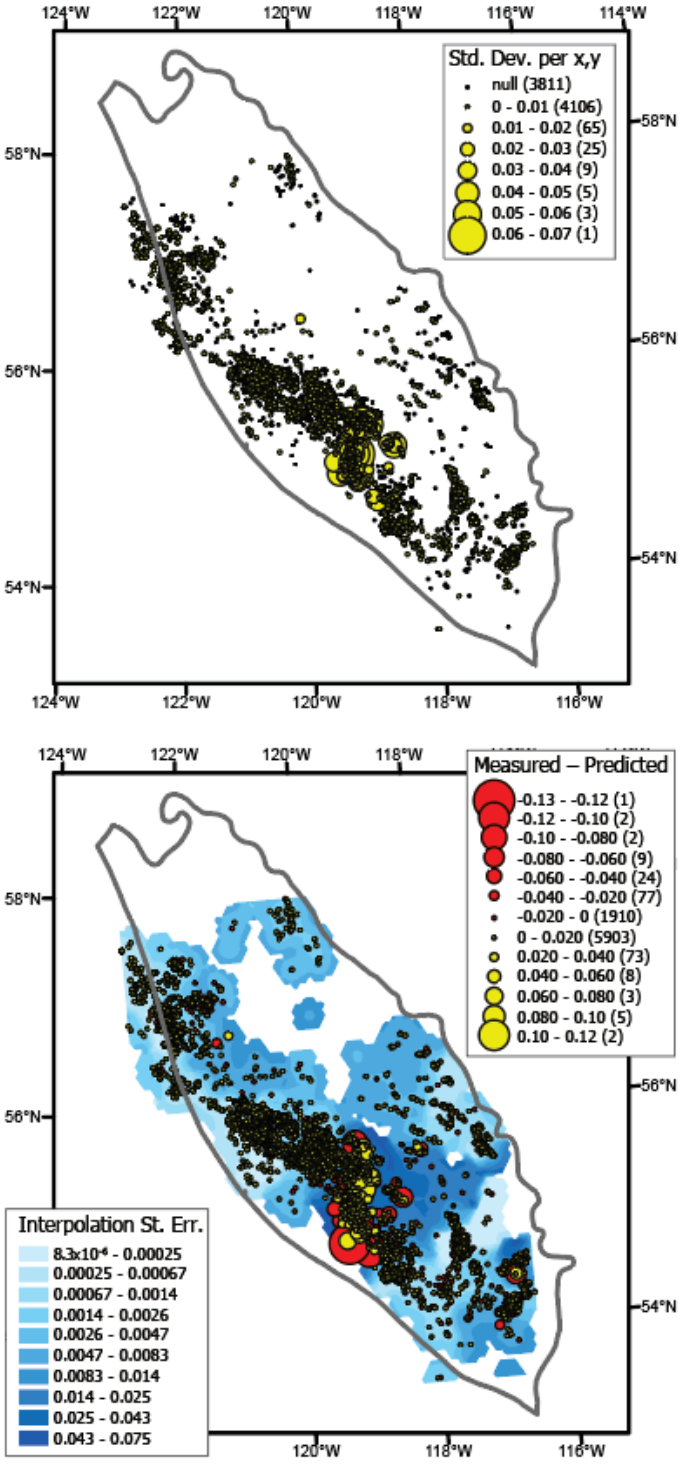

Figure 8. (A) Standard deviations of H_2S in the gas-phase for each X-Y location with number of values for each interval shown in parentheses. (B) Standard error uncertainty map (blue shades) with difference between measured and predicted values shown as circle where the size of the circle represent magnitude of deviation from model prediction, number of values for each interval shown in parentheses.

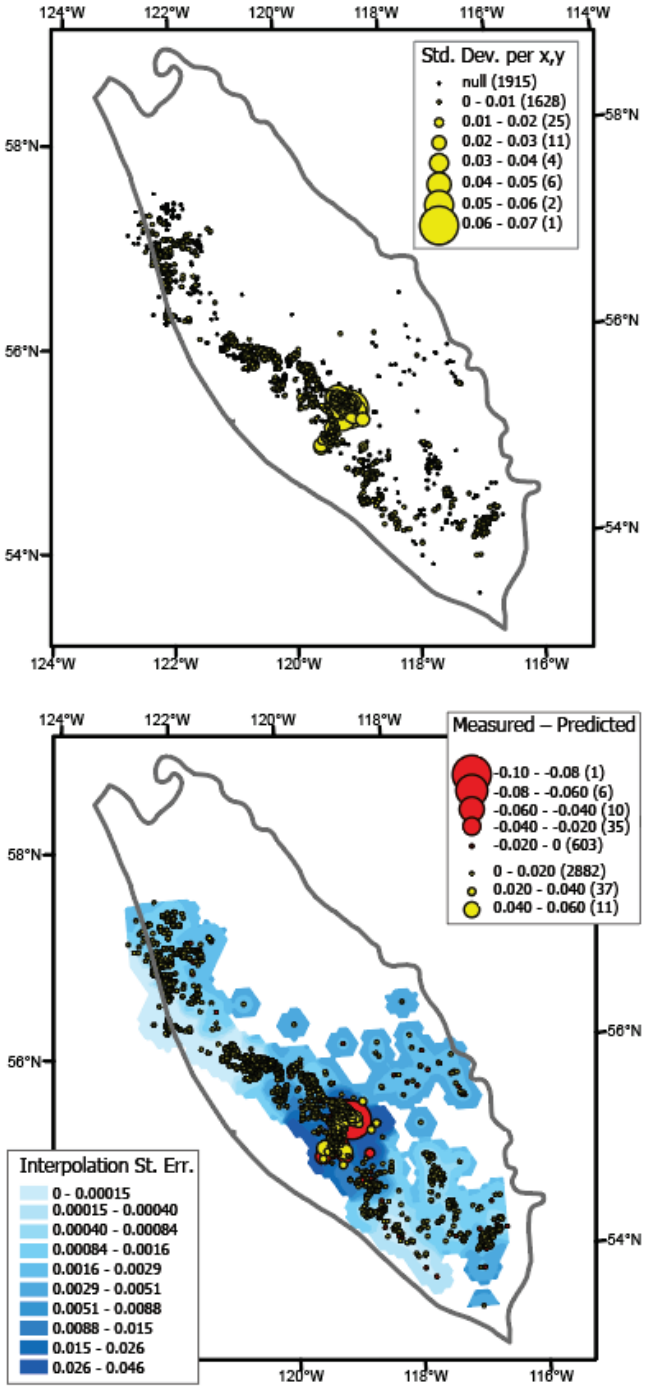

Figure 9. (A) Standard deviations of H_2S in the liquid-phase for each X-Y location with number of values for each interval shown in parentheses. (B) Standard error uncertainty map (blue shades) with difference between measured and predicted values shown as circle where the size of the circle represent magnitude of deviation from model prediction, number of values for each interval shown in parentheses.

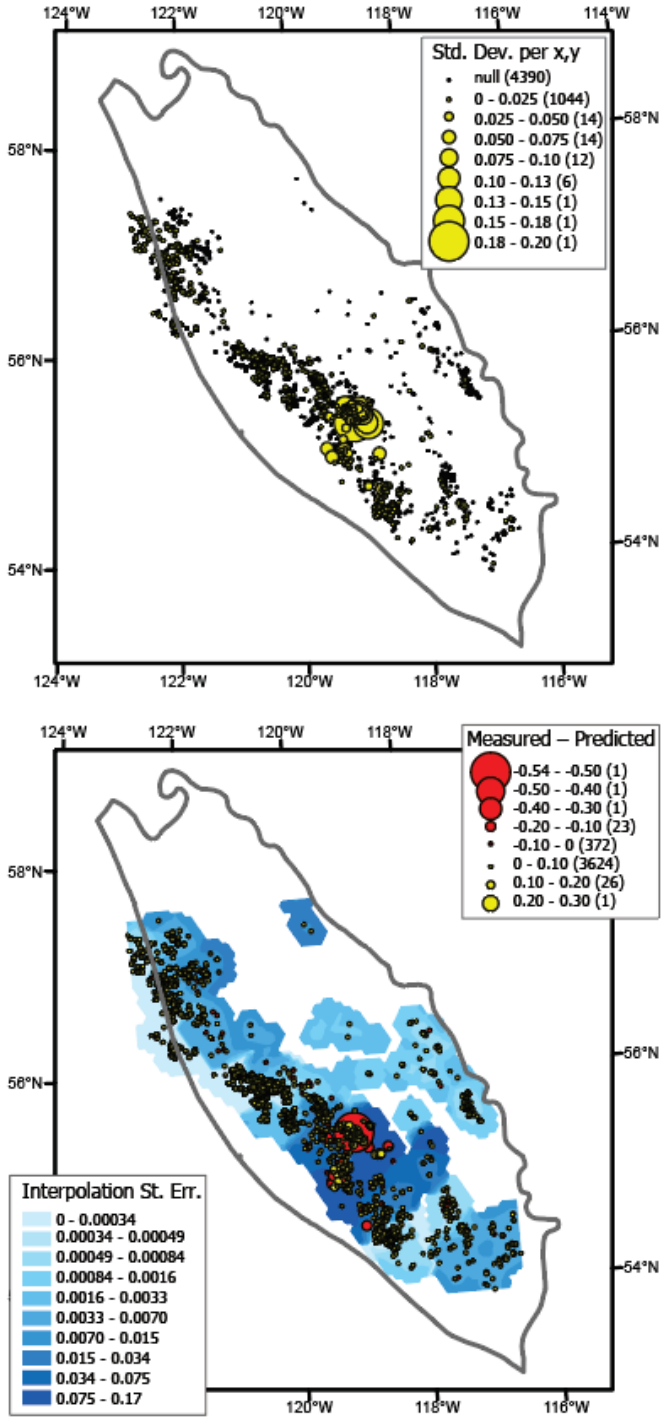

Figure 10. (A) Standard deviations of H_2S in water for each X-Y location with number of values for each interval shown in parentheses. (B) Standard error uncertainty map (blue shades) with difference between measured and predicted values shown as circle where the size of the circle represent magnitude of deviation from model prediction, number of values for each interval shown in parentheses.

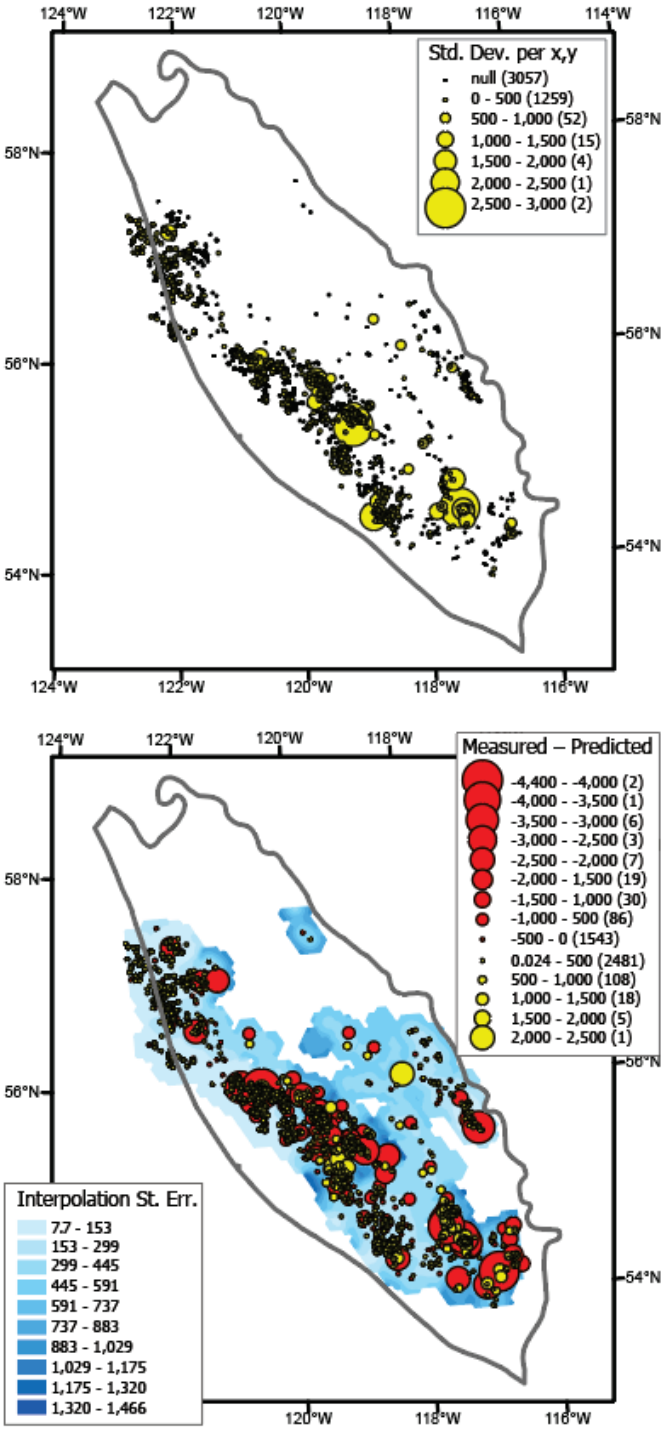

Figure 11. (A) Standard deviations of sulfate (SO_4) in water for each X-Y location with number of values for each interval shown in parentheses. (B) Standard error uncertainty map (blue shades) with difference between measured and predicted values shown as circle where the size of the circle represent magnitude of deviation from model prediction, number of values for each interval shown in parentheses.

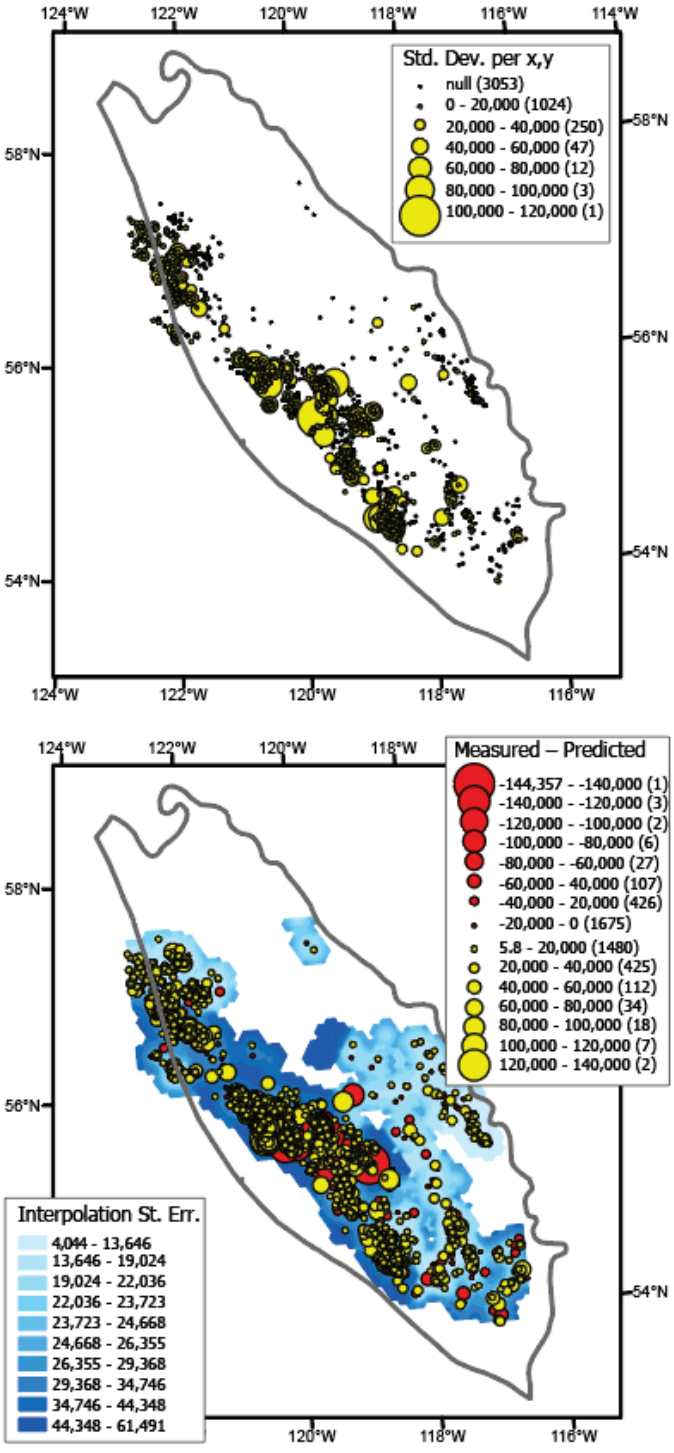

Figure 12. (A) Standard deviations of chloride (Cl) in water for each X-Y location with number of values for each interval shown in parentheses. (B) Standard error uncertainty map (blue shades) with difference between measured and predicted values shown as circle where the size of the circle represent magnitude of deviation from model prediction, number of values for each interval shown in parentheses.